Journal of Solid State Chemistry **144,** 16–19 (1999)
Article ID jssc.1998.8029, available online at http://www.idealibrary.com on IDEAL®

Rietveld Refinement of the Crystal Structure of Cs(IV), a *d*-Electron Metal

J. L. Delattre[1] and J. V. Badding

Pennsylvania State University, University Park, Pennsylvania 16802
E-mail: jbadding@chem.psu.edu

Received April 22, 1998; in revised form September 11, 1998; accepted September 15, 1998

Rietveld refinement of the crystal structure of the high-pressure phase Cs(IV) is described. Cs(IV) has a transition metal-like electronic structure that influences its open-packed crystal structure, which consists of trigonal prisms of Cs atoms. The structure was refined with reliability factors $R_F^2 = 0.050$, $R_{wp} = 0.043$, and $R_p = 0.032$ in space group $I4_1/amd$ with the cesium atoms in the 4a position. © 1999 Academic Press

I. INTRODUCTION

Cs(IV) is a high-pressure phase of cesium that is a d^1 metal with an extraordinary bonding configuration. Beginning at a pressure of 4.2 GPa, there is an *s*-to-*d* electronic transition in cesium (1–3), which also occurs in other compressible elements (3). The transition has a major impact on the crystal structure of Cs(IV) (which is stable from 4.3 to 10 GPa), making it more open and directional as a result of the more localized, covalent-like *d*-electron bonding (4). Because *d* electrons have minimal electron density at the nucleus and maximal electron density away from the nucleus, it has been proposed that Cs(IV) can be considered an electride, consisting of Cs^+ ions and electrons (5). This view of the electronic structure is supported by preliminary electronic structure calculations, which suggest that Cs(IV) can be viewed as isostructural to the Zintl compound α-$ThSi_2$ with the Cs atoms located in the Th positions and some of the Cs(IV) valence electron density maxima located in the silicon positions (5). These conclusions must be based on an accurate knowledge of the crystal structure of Cs(IV).

A body-centered tetragonal ($I4_1/amd$) crystal structure has been proposed for Cs(IV) with lattice parameters $a = 3.349(6)$ Å, $c = 12.49(3)$ Å at 8.0 GPa (4). This structure was determined by inspection of high-pressure powder X-ray crystallographic data. Further investigation by means of energy dispersive synchrotron diffraction techniques confirmed the assignment of a tetragonal lattice for Cs(IV) (6). In these investigations, the integrated diffraction intensities were not accurate due to the presence of insufficiently small cesium crystallites and/or substantial amounts of preferred orientation. Because of these uncertainties, which are typical for many high-pressure crystallographic investigations, it is important to have quantitative verification of the crystal structure of Cs(IV). We have developed techniques to obtain higher resolution laboratory-based high-pressure diffraction data as well as reduce the crystallite size in metals such as cesium that readily form large crystallite grains (7, 8). Here we report the verification of the crystal structure of Cs(IV) by means of Rietveld refinement of new diffraction data.

II. EXPERIMENTAL

Samples were loaded into a modified Merril–Bassett diamond-anvil cell under a high-purity argon atmosphere. A 250-μm sample hole and a T301 stainless steel gasket were used. Powder diffraction patterns were collected at high pressure by means of a diffraction system that utilizes a Johannson–Guinier monochromator to focus an X-ray beam (Mo$K\alpha_1$, $\lambda = 0.7093$ Å) from a Rigaku RU-200H rotating anode generator onto the sample. The $K\alpha_2$ component is reduced to approximately 10 to 15% of the $K\alpha_1$ component. The radiation is focused in the horizontal plane (7). The beam is collimated to 75 μm in the vertical plane in which diffraction information is collected. Diffraction data were collected on pure cesium (99.99%) and cesium mixed with amorphous boron powder (99.99%) in a 1:1 ratio by mass. The presence of amorphous boron, which contributes minimally to the observed diffraction pattern, reduces the crystallite size and the effects of preferred orientation. The diffraction patterns were collected on Kodak DEF-392 film at pressures ranging from 7 to 13.3 GPa. A 50-μm-radius film cassette was used. The two-dimensional diffraction pattern was scanned into a Macintosh computer and collapsed into a one-dimensional profile using the program of Meade

[1]Present address: Department of Chemistry, University of California at Berkeley, Berkeley, CA 94720.

0022-4596/99 $30.00

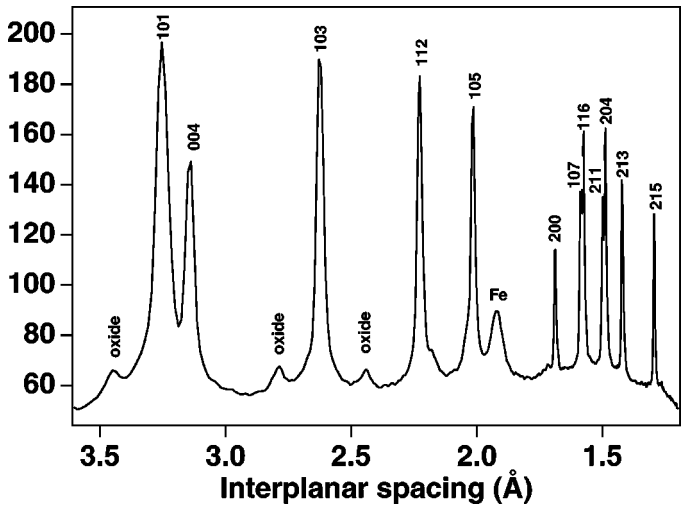

FIG. 1. Diffraction pattern for elemental cesium at 9.0 GPa.

et al. (9). Data collection times were 13 h for the pure cesium sample and 21 h for the cesium–boron mixture. Pressures were determined by the shift of the ruby R_1 line.

III. STRUCTURE REFINEMENT

The diffraction pattern for pure Cs(IV) at 9.0 GPa (Fig. 1) contains small peaks at interplanar spacings of 3.45, 2.79, and 2.44 Å from cesium oxide impurities and a peak at 1.92 Å from the stainless steel gasket. The resolution of this pattern is considerably improved when compared with earlier reported patterns. For example, two previously unresolved pairs of closely spaced lines were resolved: the 107 and 116 lines and the 211 and 204 lines (Fig. 1). The figure of merit (10) $M(12)$ for the 12 lines with the largest interplanar spacings was 50, indicating that the tetragonal indexing is correct.

As in previous studies, the intensity profile collected for the pure cesium sample was inaccurate. After mixing with boron, the diffraction ring profiles on the film were smooth, indicating that many crystallites contributed to the diffraction pattern. The presence of boron in the mixture also broadened the diffraction peaks (Fig. 2) due to the increased amount of nonhydrostatic stress that arises because boron is stronger than cesium. However, this did not preclude structure refinement.

Using the previously proposed structural model (4) and the program GSAS (11), Rietveld refinement was performed on diffraction data from the cesium–boron mixture (Fig. 2). The intensities were corrected for the nonlinear relationship between the film density and exposure (8). The step size for the digitized profile was 0.031 Å. The oxide and iron impurity peaks in the regions $2\theta = 16.6$–17.5° and 21.1–22.2 Å were excluded during refinement. The refined parameters included scale, background, lattice, preferred orientation, and isotropic thermal parameters. Both the predominant Mo$K\alpha_1$ and the minor Mo$K\alpha_2$ X-ray components were included in the refinement. The peak shapes were modeled using the pseudo-Voight profile function of Thompson *et al.* (12). The preferred orientation models of both Popa (13)

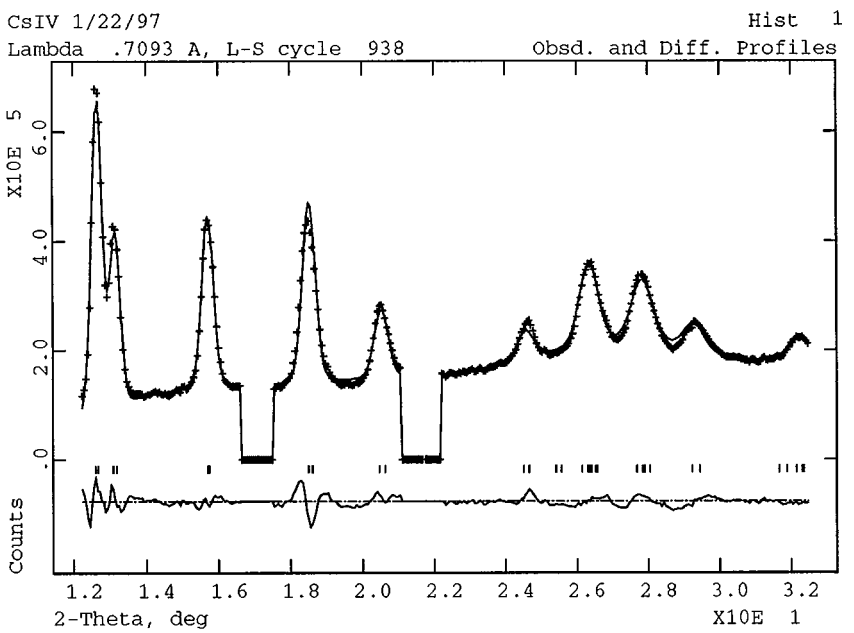

FIG. 2. Observed, calculated, and difference profiles determined by Rietveld analysis for elemental cesium mixed with amorphous boron at 13.3 GPa.

TABLE I
Crystallographic Data at 20°C and 13.3 GPa

$a = 3.3366(4)$ Å
$c = 12.408(2)$ Å
$V = 138.14$ Å
Space group: $I4_1/amd$
$Z = 4$
$d_c = 6.390$ g/cm^3
$B_{iso} = 0.018(1)$ Å^2
Atomic position: 4*a*
Interatomic distances: Cs–4Cs = 3.37 Å, Cs–4Cs = 3.52 Å

and March and Dollase (14) were used. Both models gave similar reliability factors, which were $R_{wp} = 0.0431$, $R_p = 0.0321$, $\chi_2 = 0.62$, and $R_F^2 = 0.050$. The amount of preferred orientation was greatly reduced by the presence of the amorphous boron. For example, the preferred orientation ratio obtained with the Dollase–March model was 0.95, which is close to the ratio of 1 obtained when there is no preferred orientation. Crystallographic and structural parameters are in Table 1.

IV. DISCUSSION

The most striking feature of the Cs(IV) structure are the trigonal prisms that arise because of the more directional and covalent *d*-electron bonding (Fig. 3). This bonding configuration is very different from that of the three cesium phases stable at lower pressures: bcc Cs(I), fcc Cs(II), and fcc Cs(III) (3). The coordination number of the cesium atoms in Cs(IV) is eight, with four nearest neighbors at a distance of 3.37 Å and four next nearest neighbors in the *a*–*b* plane at 3.52 Å (Fig. 3). The radius of the Cs atoms derived from the nearest neighbor distance is 1.69 Å, comparable to the ionic radius of Cs at ambient pressure, 1.67 Å (15). (It is interesting to note that at higher pressures the radius of Cs becomes smaller than that of xenon (3), which is isolectronic with Cs^+. This is likely due to the stronger d-electron bonding in Cs.) Assuming this atomic radius, the packing fraction in Cs(IV) at 13.3 GPa is 58%, considerably less than the packing fraction of bcc cesium (68%) at ambient pressure or the two fcc high-pressure cesium phases (72%). Even though there is a dramatic decrease in packing fraction associated with the transition to a more open, covalent structure, the overall molar volume of cesium decreases because of the rapid decrease in atomic size (4). These changes in the size and electronic structure of elemental cesium should have a major impact on its chemical behavior (16).

Finally, the crystal structure of the high-pressure phase Cs(V), which is also open-packed as a result of *d*-electron bonding (but appears more complex than the structure of Cs(IV)), remains unsolved (17). Rietveld refinement techniques such as those described here should prove useful in the solution of this structure and related structures of other compressible metals.

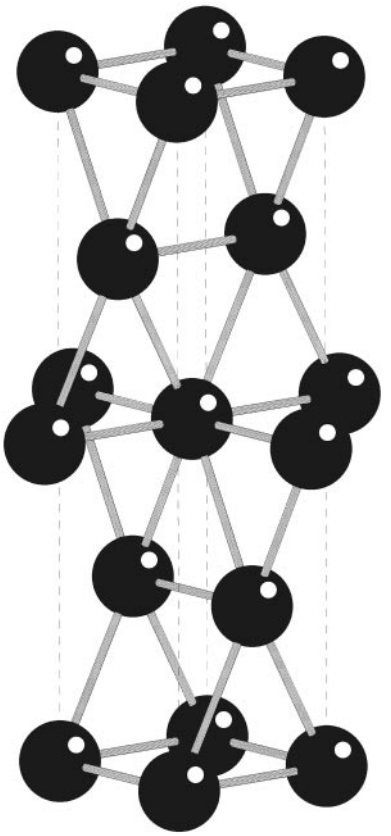

FIG. 3. Crystal structure of Cs(IV) at 13.3 GPa. The tetragonal *c* axis is vertical. Some of the cesium atoms have been removed for clarity. The structure can be constructed from trigonal prisms of cesiums. The eight-coordination about a single cesium can be seen for the central body-centered atom. The nearest neighbor bonds (four) that are in the *a*–*b* plane are 3.37 Å long. All of the other nearest neighbor bonds (four) that are not in the *a*–*b* plane are 3.52 Å long.

ACKNOWLEDGMENTS

This work was supported by a NSF Young Investigator award and the donors Petroleum Research Fund, administered by the American Chemical Society. J. L. D. thanks M. Hasegawa and L. J. Parker for helpful discussions on Rietveld analysis and powder diffraction.

REFERENCES

1. H. G. Drickamer, *in* "Solid State Physics" (F. Seitz and D. Turnbull, Eds.), p. 1. Academic Press, New York, 1965.
2. R. M. Sternheimer, *Phys. Rev.* **78,** 235 (1950).
3. D. A. Young, "Phase Diagrams of the Elements," Univ. of California Press, Berkeley, 1991.

4. K. Takemura, S. Minomura, and O. Shimomura, *Phys. Rev. Lett*. **49,** 1772 (1982).
5. H. G. von Schnering and R. Nesper, *Angew. Chem.* **26,** 1059 (1987).
6. J. V. Badding, H. K. Mao, and R. J. Hemley, *Soild State Comm.* **77,** 801 (1991).
7. T. Atou and J. V. Badding, *Rev. Sci. Instrum.* **66,** 4496 (1995).
8. M. Hasegawa and J. V. Badding, *Rev. Sci. Instrum.* **68,** 2298 (1997).
9. J. Nguyen and R. Jeanloz, *Rev. Sci. Instrum.* **64,** 3456 (1993).
10. A. D. Mighell, C. R. Hubbard, J. K. Stalick, and M. A. Holomany, "NBS* AIDS83: A Manual Describing the Data Format Used in NBS* AIDS83." JCPDS-International Centre for Diffraction Data, Swarthmore, PA, 1983.
11. A. C. Larson and R. B. Von Dreele, "GSAS: General Structure Analysis System," Report LAUR 86-748. Los Alamos National Laboratory, Los Alamos, NM, 1994.
12. P. Thompson, D. E. Cox, and J. B. Hastings, *J. Appl. Crystallogr*. **20,** 79 (1987).
13. N. C. Popa, *J. Appl. Crystallogr*. **25,** 611 (1992).
14. Dollase, *J. Appl. Crystallogr*. **19,** 267 (1986).
15. N. N. Greenwood and A. Earnshaw, "Chemistry of the Elements." Pergamon, Oxford, 1984.
16. J. V. Badding, L. J. Parker and D. A. Nesting, *J. Solid State Chem.* **117,** 229 (1995).
17. K. Takemura and K. Syassen, *Phys. Rev. B* **32,** 2213 (1985).